REMUNOM
ISSN 2178-6925

Received: 15/10/2026 - **Accepted:** 09/11/2026
Vol: 13.23
DOI: 10.66104/zkvyrq84
Pages: 1-31

INFLUÊNCIA DO TEMPO DE TRATAMENTO E DA VAZÃO DE NITROGÊNIO SOBRE O ÍNDICE DE DENSIDADE E O POTENCIAL DE POROSIDADE DA LIGA DE ALUMÍNIO AA 380.0 PARA INJEÇÃO SOB ALTA PRESSÃO

INFLUENCE OF TREATMENT TIME AND NITROGEN FLOW RATE ON THE DENSITY INDEX AND POROSITY POTENTIAL OF AA 380.0 ALUMINUM ALLOY FOR HIGH-PRESSURE DIE CASTING

INFLUENCIA DEL TIEMPO DE TRATAMIENTO Y DEL CAUDAL DE NITRÓGENO SOBRE EL ÍNDICE DE DENSIDAD Y EL POTENCIAL DE POROSIDAD DE LA ALEACIÓN DE ALUMINIO AA 380.0 PARA FUNDICIÓN A PRESIÓN

Rodrigo S. Rodrigues
IFRS, Federal Institute of Education, Science and Technology of Rio Grande do Sul (IFRS), Caxias do Sul, RS, Brazil
E-mail: rodrigo.salib01@gmail.com

Juliano C. Toniolo
IFRS, Federal Institute of Education, Science and Technology of Rio Grande do Sul (IFRS), Caxias do Sul, RS, Brazil
E-mail: juliano.toniolo@caxias.ifrs.edu.br

Resumo

Foi conduzido um planejamento fatorial completo 3^2 com duas repetições, totalizando 18 ensaios experimentais. A qualidade metalúrgica foi quantificada pelo Índice de Densidade (ID), determinado pelo método hidrostático após o teste de pressão reduzida (RPT). O ID reduziu de 27,6 % (banho sem tratamento) para 0,90 % após 720 s de desgaseificação. A modelagem por Metodologia de Superfície de Resposta (MSR) ajustou um polinômio de segunda ordem (R^2 = 98,54 %; R^2 ajustado = 97,94 %; R^2 previsto = 96,87 %), confirmando a significância estatística do tempo, da vazão e da interação tempo×vazão ($p < 0,05$). A análise termodinâmica baseada na Lei de Sieverts mostrou redução de 36 % na solubilidade de equilíbrio do hidrogênio devido à queda térmica do banho (787 °C → 711 °C). Os menores valores experimentais de ID foram observados em T = 720 s e V ≈ 25 L/min.

Palavras-chave: Liga de alumínio AA 380.0; fundição sob alta pressão; desgaseificação com nitrogênio; Índice de Densidade; metodologia de superfície de resposta.

CC BY

REMUNOM
ISSN 2178-6925

Received: 15/10/2026 - **Accepted:** 09/11/2026
Vol: 13.23
DOI: 10.66104/zkvyrq84
Pages: 1-31

Abstract

A complete 3² factorial design was conducted with two replicates, totaling 18 experimental runs. The metallurgical quality was quantified by the Density Index (DI), determined by the hydrostatic method after a reduced pressure test (RPT). The DI reduced from 27.6 % (untreated bath) to 0.90 % after 720 s of degassing. Response Surface Methodology (RSM) modeling adjusted a second-order polynomial (R^2 = 98.54 %; adjusted R^2 = 97.94 %; predicted R^2 = 96.87 %), confirming statistical significance of time, flow, and time×flow interaction ($p < 0.05$). The thermodynamic analysis based on Sieverts' Law showed a 36 % reduction in the equilibrium solubility of hydrogen due to the thermal drop of the bath (787 °C → 711 °C). The lowest experimental DI values were observed at T = 720 s and V ≈ 25 L/min.

Keywords: AA 380.0 aluminum alloy; high-pressure die casting; nitrogen degassing; Density Index; response surface methodology.

Resumen

Se realizó un diseño factorial completo 3² con dos repeticiones, totalizando 18 ensayos experimentales. La calidad metalúrgica se cuantificó mediante el Índice de Densidad (ID), determinado por el método hidrostático tras la prueba de presión reducida (RPT). El ID se redujo de 27,6 % (baño sin tratamiento) a 0,90 % tras 720 s de desgasificación. El modelado por Metodología de Superficie de Respuesta (MSR) ajustó un polinomio de segundo orden (R^2 = 98,54 %; R^2 ajustado = 97,94 %; R^2 predicho = 96,87 %), confirmando la significancia estadística del tiempo, del caudal y de la interacción tiempo×caudal ($p < 0,05$). El análisis termodinámico basado en la Ley de Sieverts mostró una reducción del 36 % en la solubilidad de equilibrio del hidrógeno debido a la caída térmica del baño (787 °C → 711 °C). Los menores valores experimentales de ID se observaron en T = 720 s y V ≈ 25 L/min.

Palabras clave: Aleación de aluminio AA 380.0; fundición a presión; desgasificación con nitrógeno; Índice de Densidad; metodología de superficie de respuesta.

1. Introduction

High-pressure die casting (HPDC) is widely used to manufacture geometrically complex aluminum components at high production rates. Its performance, however, is strongly affected by melt quality because gas porosity, oxide films, and entrained air can reduce structural integrity and leak tightness (ANYALEBECHI, 2022; GYARMATI et al., 2021).

Although rotary degassing units are widely discussed in recent literature, injection remains relevant in industrial furnaces where simpler equipment is used. The practical question is therefore not only whether degassing reduces porosity potential, but how treatment time and nitrogen flow interact within the operating range of a rotary degassing system.

This study evaluates the effects of degassing time and nitrogen flow rate on the RPT-based DI of AA 380.0 alloy using a replicated 3² factorial design and response-surface analysis. The scope is limited to process-level porosity-potential

CC BY

REMUNOM
ISSN 2178-6925

Received: 15/10/2026 - **Accepted:** 09/11/2026
Vol: 13.23
DOI: 10.66104/zkvyrq84
Pages: 1-31

reduction. Direct hydrogen measurement, Bifilm Index determination, K-mold testing, radiography of finished parts, and mechanical validation were not performed.

2. Literature Review

Hydrogen is the principal gas dissolved in liquid aluminum. Its solubility decreases sharply during solidification, so hydrogen rejected from solution can contribute to pore formation. Porosity in aluminum castings is nevertheless multicausal: dissolved hydrogen, solidification shrinkage, entrained air, and oxide bifilms may interact during filling and solidification (ANYALEBECHI, 2022; KANG et al., 2025; SAMUEL et al., 2023; VANDER VOORT, 2007). Consequently, the Reduced Pressure Test (RPT) and Density Index (DI) should be interpreted as indicators of porosity potential rather than as direct measurements of hydrogen concentration or inclusion cleanliness (SAMUEL et al., 2023; VANDER VOORT, 2007).

Inert-gas degassing reduces dissolved hydrogen by transferring it from the melt to rising gas bubbles. Treatment efficiency depends on residence time, gas flow rate, bubble population, gas–metal interfacial area, bath temperature, and the hydrodynamics of the injection device (DISPINAR; CAMPBELL, 2004b; ENGH, 1992). Rotary systems generally promote finer bubble dispersion, whereas RDU may generate larger and less uniformly distributed bubbles; excessive gas flow may also increase turbulence, reoxidation, and entrainment (DISPINAR; CAMPBELL, 2004b; ENGH, 1992).

Recent studies have reported the dependence of DI and melt quality on degassing time, treatment configuration, and filtration conditions in Al–Si alloys (DISPINAR; CAMPBELL, 2004a; TALBOT; ANYALEBECHI, 1988). These studies support the use of DI for comparative process monitoring while also showing that DI alone does not isolate the individual contributions of hydrogen, bifilms, shrinkage, and entrained air. A combined assessment using direct hydrogen measurement and/or a Bifilm Index can therefore provide a broader characterization of melt quality (DISPINAR; CAMPBELL, 2004a; SAMUEL et al., 2023; VANDER VOORT, 2007).

CC BY

REMUNOM
ISSN 2178-6925

Received: 15/10/2026 - **Accepted:** 09/11/2026
Vol: 13.23
DOI: 10.66104/zkvyrq84
Pages: 1-31

3. Methodology

The material used in this study was a cast aluminum alloy classified as AA 380.0, belonging to the Al-Si-Cu system, equivalent to the designation AA 380.0 (UNS A13800), according to the standard ASTM B85/B85M-18 — Standard Specification for Aluminum-Alloy Die Castings (ASTM INTERNATIONAL, 2018). This alloy is widely used in High-Pressure Die Casting (HPDC) processes and is characterized by good fluidity, high filling capacity for complex molds and mechanical properties suitable for structural applications and components subject to thermal and mechanical stresses, such as automotive systems.

The chemical composition of the charge was measured by optical emission spectrometry and is summarized in Table 1. The measured composition was within the limits specified for AA 380.0 in standard ASTM B85/B85M-18 (ASTM INTERNATIONAL, 2018). Titanium was not detected/reported in the available spectrometry record and is therefore identified as not reported (NR).

Table 1. Chemical composition of the AA 380.0 aluminum alloy used in this study and compliance with ASTM B85/B85M-18 (ASTM INTERNATIONAL, 2018)

Element	Measured Content (wt.%)	ASTM B85/B85M-18 Limit (wt.%)	Compliance
Si	8.7 ± 0.2	7.5 – 9.5	Within specification
Cu	3.4 ± 0.1	3.0 – 4.0	Within specification
Fe	0.9 ± 0.1	≤ 1.3	Within specification
Zn	1.2 ± 0.1	≤ 3.0	Within specification
Mn	0.3 ± 0.05	≤ 0.5	Within specification
Mg	0.08 ± 0.02	≤ 0.1	Within specification
Ti	NR	≤ 0.20	Not reported
Ni	NR	≤ 0.50	Not reported
Sn	NR	≤ 0.35	Not reported

The use of experimental designs for optimization of process parameters in aluminum alloys has been widely adopted in the recent literature. Merchan et al. (2025) applied Design of Experiments (DoE) in the optimization of HPDC parameters for Al-Mg-Fe alloys, demonstrating the effectiveness of the methodology for identifying statistically significant variables and reducing porosity.

CC BY

REMUNOM
ISSN 2178-6925

Received: 15/10/2026 - **Accepted:** 09/11/2026
Vol: 13.23
DOI: 10.66104/zkvyrq84
Pages: 1-31

The theoretical density of the AA 380.0 (AA 380) alloy in the solid state is approximately 2.74 g/cm³, being used only as a metallurgical and comparative reference of the alloy. However, a constant theoretical density was not used for the calculation of the Density Index (DI); the actual density of the solidified sample under atmospheric pressure (D_{atm}) was used, experimentally determined by the hydrostatic method for each condition analyzed. This approach avoids the introduction of systematic error in the DI, since the index must represent the relative difference between the sample solidified under atmospheric pressure and the sample solidified under reduced pressure of the same experimental condition.

The determination of the apparent density of the samples was carried out by means of the hydrostatic method, following the principles established by the ASTM B962 (ASTM INTERNATIONAL, 2023) standard, used to evaluate the density of metallic materials by fluid displacement, ensuring greater reliability and repeatability of the experimental measurements.

To carry out the experiments, a load of approximately 400 kg of the alloy was melted in an induction furnace. The use of this type of furnace allows for a more uniform heating of the metal bath, in addition to favoring precise temperature control and reducing external contamination. During melting, conventional aluminum metallurgy practices were adopted, including the removal of surface slag (dross) and the minimization of bath exposure to the atmosphere, with the aim of limiting oxidation and the formation of aluminum oxides (Al_2O_3), which can act as nucleation sites for internal defects. To minimize hydrogen pickup and oxidation during melting, the furnace door was kept closed whenever possible, dross was removed immediately prior to degassing, sampling operations were performed as rapidly as practicable, and unnecessary bath agitation was avoided. No flux cover or protective atmosphere was employed.

Therefore, controlling the melt conditions before casting, especially through degassing processes, is essential to ensure the quality of the material. In the present study, special attention was given to the preparation of the liquid metal, ensuring reproducible conditions for the application of experimental design.

CC BY

REMUNOM
ISSN 2178-6925

Received: 15/10/2026 - **Accepted:** 09/11/2026
Vol: 13.23
DOI: 10.66104/zkvyrq84
Pages: 1-31

Bath temperature was monitored and maintained within the industrial operating range; however, a gradual temperature decrease occurred during the experimental sequence, as presented in Section 4.2. The study was conducted through a structured experimental design (Design of Experiments – DOE), with the objective of evaluating the influence of degassing parameters on the quality of liquid aluminum, focusing on reduction in RPT-based porosity potential efficiency.

Degassing was performed using an industrial Rotary Degassing Unit (RDU) positioned at the center of the molten AA 380.0 bath. The rotor was immersed to a depth of 300 mm and operated continuously at 400 rpm throughout all experimental runs. Nitrogen was injected through the rotor assembly at the specified flow rates (15, 25, and 30 L/min). Rotor speed, immersion depth, and rotor geometry were maintained constant for all experiments. Nitrogen purity was not documented in the available experimental record and is therefore reported as a methodological limitation rather than inferred. The bath temperature was monitored with a thermocouple during the experimental sequence. Melt quality was assessed by RPT followed by hydrostatic density measurement. No direct hydrogen measurement or K-mold cleanliness test was performed.

A complete 3^2 factorial design was adopted, including the following two factors:

- Degassing time (seconds);
- Inert gas flow rate (L/min).

Each factor was evaluated at three levels, resulting in a total of 9 distinct experimental conditions. To increase the reliability of the results and allow the estimation of the experimental error, two independent replicates were performed for each condition, totaling 18 experimental trials.

Table 2. Experiment input data

Run	Time (s)	Flow rate (L/min)	Replicate
1	300	15	1
2	300	15	2
3	300	25	1
4	300	25	2
5	300	30	1
6	300	30	2

CC BY

REMUNOM
ISSN 2178-6925

Received: 15/10/2026 - **Accepted:** 09/11/2026
Vol: 13.23
DOI: 10.66104/zkvyrq84
Pages: 1-31

Run	Time (s)	Flow rate (L/min)	Replicate
7	480	15	1
8	480	15	2
9	480	25	1
10	480	25	2
11	480	30	1
12	480	30	2
13	720	15	1
14	720	15	2
15	720	25	1
16	720	25	2
17	720	30	1
18	720	30	2

The executions were carried out in a randomized manner, with the objective of minimizing the influence of uncontrolled variables, such as thermal variations of the bath or environmental conditions. Between each test, consistent operating conditions were maintained, ensuring the repeatability of the process.

The experimental procedure consisted of the following steps:

- **Preparation of the metal bath:** after the complete melting of the AA 380.0 alloy, the bath was stabilized at the previously defined processing temperature, ensuring thermal and chemical homogeneity.
- **Application of degassing:** for each experimental condition, nitrogen gas was injected into the metal bath, according to the defined time and flow levels. The gas was introduced in a controlled manner, promoting the formation of bubbles and the reduction in porosity potential associated with gas treatment by a mechanism of diffusion and drag.
- **Sample collection:** at the end of the degassing process, samples of the liquid metal were collected and solidified under controlled conditions, in order to preserve the metallurgical characteristics of the treated material.
- **Replicate runs:** each experimental condition was repeated twice independently, ensuring the evaluation of the variability of the process and allowing greater statistical robustness in the analysis of the results.

CC BY

REMUNOM
ISSN 2178-6925

Received: 15/10/2026 - **Accepted:** 09/11/2026
Vol: 13.23
DOI: 10.66104/zkvyrq84
Pages: 1-31

The use of replicates in the experimental design was fundamental for the estimation of pure error and for the application of statistical techniques, enabling the identification of the significance of the factors studied and their interactions.

In addition, the use of a complete factorial DOE allowed not only the evaluation of the main effects of time and flow, but also the analysis of the possible interaction between these factors, a relevant aspect considering that the efficiency of degassing depends on coupled phenomena of mass transfer and bubble dynamics in the metal bath.

A single molten bath of approximately 400 kg of AA 380.0 alloy was used throughout the experimental campaign. The experimental conditions were performed sequentially according to the randomized DOE matrix. Before each run, the molten bath was reconditioned by temperature adjustment and homogenization to maintain stable process conditions. Replicates were conducted as independent experimental runs under the same treatment parameters, with new degassing operations, independent sampling, and independent RPT density measurements. Therefore, the replicate observations represent independent process realizations rather than repeated measurements of the same specimen.

Bath temperature was recorded during all experimental runs; however, temperature was not included as a DOE factor or statistical covariate because the original experimental design was limited to treatment time and nitrogen flow rate. The influence of temperature was therefore evaluated qualitatively and is discussed separately in Section 4.2.

3.1 Reduced Pressure Test and Density Index

The efficiency of the degassing process was evaluated by determining the apparent density of the samples and visual analysis of the porosity, using the *Reduced Pressure Test (RPT)* method, a technique widely used for indirect estimation of the hydrogen content in liquid aluminum alloys.

3.2 Experimental configuration and degassing procedure

The RDU rotor was maintained at the center of the bath with a constant immersion depth of 300 mm throughout all runs. Nitrogen exited through four 2 mm

CC BY

REMUNOM
ISSN 2178-6925

Received: 15/10/2026 - **Accepted:** 09/11/2026
Vol: 13.23
DOI: 10.66104/zkvyrq84
Pages: 1-31

diameter holes. These geometric parameters were held constant to reduce hydrodynamic variability.

Figure 1 shows the industrial degassing equipment used in this study. The system consists of a submerged rotary rotor mounted on a movable support structure for nitrogen injection into the molten aluminum bath. The equipment was used to perform the degassing treatments according to the experimental design, varying treatment time and gas flow rate.



Fig. 1. Industrial rotary degassing unit (RDU) used for nitrogen injection and melt treatment of the AA 380.0 aluminum alloy during the experimental campaign.

Before carrying out the tests, the operational conditions of the equipment used were verified, in order to ensure the reliability and repeatability of the measurements, in accordance with the technical competence requirements established by the ISO/IEC 17025:2017 standard — General requirements for the competence of testing and calibration laboratories (ISO, 2017). All measuring instruments used in the tests had valid calibration certificates traceable to standards recognized by the International System of Units (SI), according to the metrological guidelines of that standard.

For the vacuum gauge, the following were evaluated:

- validity of the calibration certificate and metrological traceability;
- power supply conditions;

CC BY

REMUNOM
ISSN 2178-6925

Received: 15/10/2026 - **Accepted:** 09/11/2026
Vol: 13.23
DOI: 10.66104/zkvyrq84
Pages: 1-31

- cleanliness and absence of dirt on the sealing surface of the chamber;
- O-ring integrity and compliance.

For the density balance (hydrostatic method), the following were verified:

- validity of the calibration certificate, with measurement uncertainty compatible with the resolution required by the test;
- presence of deionized water in the system;
- proper leveling of the equipment;
- absence of external vibrations that could interfere with the measurement.

In addition, the measuring room was maintained under controlled environmental conditions, with a temperature of 20 ± 3 °C and relative humidity below 75%, in compliance with the good metrological practices recommended by ISO/IEC 17025:2017 (ISO, 2017), ensuring that the environmental conditions did not compromise the validity of the results obtained.

3.3 Reduced Pressure Test and density determination

The samples were obtained immediately after the degassing process, following the procedure described below:

The RPT chamber was operated at 80 ± 5 mbar absolute pressure. The value was monitored during the test cycle and recorded before sample solidification. The mold was preheated to remove residual moisture and reduce thermal gradients before pouring the liquid metal. The inner mold surface was lubricated with a graphite-based release agent (ALUFLOW 350T or Alfa Flux AL12) to facilitate sample extraction and prevent adhesion.

The degassed liquid aluminum was collected and poured into the mold. Because entrained air can affect RPT density in addition to hydrogen and shrinkage, the operator minimized turbulence during sampling and pouring. The exact free-fall height was not recorded; therefore, a quantitative confirmation of identical minimum pouring height for every run cannot be made and is recognized as a limitation. The sample was then placed in the vacuum chamber and solidified under reduced pressure. The cycle lasted approximately 300 s.

After the end of the cycle, the sample was demolded, cooled under running water and prepared for analysis.

CC BY

REMUNOM
ISSN 2178-6925

Received: 15/10/2026 - **Accepted:** 09/11/2026
Vol: 13.23
DOI: 10.66104/zkvyrq84
Pages: 1-31

The bulk density of samples solidified under reduced pressure (D_{RPT}) and samples solidified under atmospheric pressure (D_{atm}) was determined using the hydrostatic method, based on Archimedes' principle, following the methodology described in ASTM B962-23 — Standard Test Methods for Density of Compacted or Sintered Powder Metallurgy (PM) Products Using Archimedes' Principle (ASTM INTERNATIONAL, 2023). Although originally developed for powder metallurgy products, this standard establishes standardized procedures for the determination of immersion density that are directly applicable to the evaluation of samples obtained by the RPT test in molten aluminum alloys.

For each experimental condition, two samples of the liquid metal were collected simultaneously:

a) a sample solidified under reduced pressure (~80 mbar) in the vacuum chamber as described in Section 3.3;
b) a sample solidified under atmospheric pressure (1 atm), in an identical metal mold and under the same pouring conditions.

Initially, each sample was weighed in dry condition (airborne mass, m_{air}). It was then suspended by a metal support and immersed in deionized water, and the apparent submerged mass (m_{water}) was recorded. The density was then calculated by Equation (1):

$$\rho = \left(\frac{m_{\text{air}}}{m_{\text{air}} - m_{\text{water}}}\right) \times \rho_{\text{water}} \quad (1)$$

where ρ_{water} is the density of the water at the test temperature.

To ensure measurement accuracy, readings were taken only after system stabilization, indicated by the absence of fluctuations in the balance signal, in compliance with the stabilization criteria outlined in ASTM B962-23 (ASTM INTERNATIONAL, 2023).

3.4 Density Index calculation and interpretation

The efficiency of degassing was quantified using the Density Index (DI), a comparative metric widely used in the international literature on aluminum smelting to evaluate the quality of the liquid metal (SAMUEL et al., 2023; VANDER VOORT,

CC BY

REMUNOM
ISSN 2178-6925

Received: 15/10/2026 - **Accepted:** 09/11/2026
Vol: 13.23
DOI: 10.66104/zkvyrq84
Pages: 1-31

2007). DI correlates the density difference between a sample solidified under atmospheric pressure and a sample solidified under reduced pressure, providing a dimensionless measure of the alloy's gaseous porosity potential.

The DI was calculated according to Equation (2):

$$\mathrm{DI}(\%) = \left(\frac{D_{\mathrm{atm}} - D_{\mathrm{RPT}}}{D_{\mathrm{atm}}}\right) \times 100 \qquad (2)$$

where:

- D_{atm} is the density of the solidified sample under atmospheric pressure (g/cm³);
- D_{RPT} is the density of the solidified sample under reduced pressure (~80 mbar) (g/cm³).

A lower DI indicates a lower overall porosity potential under the specified RPT conditions. DI is sensitive to dissolved hydrogen, but it may also be affected by shrinkage, entrained air, oxide films, sampling, and pouring practice; it must therefore not be interpreted as a direct hydrogen measurement.

The use of DI as the primary metric, replacing the absolute density of the RPT sample, allows a direct comparison with data from the international literature and eliminates the influence of variations in the chemical composition of the alloy on the interpretation of the results, since the calculation is normalized by the atmospheric density of the analyzed sample itself.

3.5 Process acceptance criterion and repeat-test procedure

Samples were considered approved when they simultaneously met the following criteria:

a) Density Index (DI) less than 2%, as recommended in the international literature for HPDC applications (SAMUEL et al., 2023; VANDER VOORT, 2007);
b) density of the RPT sample greater than 2.65 g/cm³; and/or
c) compliance with low porosity visual standards.

The criterion based on DI was adopted as the primary metric of acceptance, as it presents greater comparative robustness and alignment with international quality control standards in aluminum casting. Results with DI higher than 2% indicated

CC BY

REMUNOM
ISSN 2178-6925

Received: 15/10/2026 - **Accepted:** 09/11/2026
Vol: 13.23
DOI: 10.66104/zkvyrq84
Pages: 1-31

inefficiency in the degassing process, requiring the repetition of the treatment of the liquid metal.

When the process criterion was not met, the industrial procedure required a new degassing cycle followed by repeat RPT/DI evaluation. Bath temperature was monitored with a thermocouple; reheating was performed before repetition if the temperature was outside the process range.

During this process, the temperature of the metal bath was monitored, considering possible thermal losses during the analysis time. If the temperature was outside the specified range, the material was returned to the furnace for reheating before repeating the process.

4. Results and Discussion

The application of the proposed correlation to the experimental results of this study allows the classification of the metallurgical quality obtained according to internationally recognized criteria. For t = 720 s, the mean DI values ranged from 0.90 % to 1.18 %, positioning the material in Grade 1 (DI < 1 %) and Grade 2 (1 ≤ DI < 2), a range considered adequate for HPDC components subjected to high hydraulic and pneumatic tightness requirements, as described by Samuel et al. (2023) and Kang et al. (2025). It should be noted that this classification refers exclusively to the potential of gaseous porosity evaluated by the RPT, and does not replace the direct radiographic inspection of the finished part.

4.1 Evolution of Density Throughout Degassing Cycles

Table 4 presents the experimental density results obtained in the solidified samples under atmospheric pressure (D_{atm}) and under reduced pressure (D_{RPT}), as well as the Density Index (DI) calculated individually for each experimental condition. The DI was determined by the ratio $DI\ (\%) = [(D_{atm} - D_{RPT})/D_{atm}] \times 100$, using the actual atmospheric density of each condition, and not a constant theoretical density of the alloy. This methodological correction is essential, as the DI is a metric relative to the run/sample itself analyzed and should reflect the effective density variation caused by the expansion of porosity under reduced pressure.

CC BY

REMUNOM
ISSN 2178-6925

Received: 15/10/2026 - **Accepted:** 09/11/2026
Vol: 13.23
DOI: 10.66104/zkvyrq84
Pages: 1-31

Table 4. Experimental data from the 3² factorial design used in the statistical analysis of RPT density

Run	Time (s)	Flow rate (L/min)	Replicate	D_{atm} (g/cm³)	D_{RPT} (g/cm³)	DI (%)
1	300	15	1	2.701	2.538	**6.03**
2	300	15	2	2.703	2.534	**6.25**
3	300	25	1	2.704	2.541	**6.03**
4	300	25	2	2.702	2.539	**6.03**
5	300	30	1	2.705	2.543	**5.99**
6	300	30	2	2.706	2.544	**5.99**
7	480	15	1	2.708	2.601	**3.95**
8	480	15	2	2.707	2.599	**3.99**
9	480	25	1	2.710	2.610	**3.69**
10	480	25	2	2.711	2.612	**3.65**
11	480	30	1	2.712	2.631	**2.99**
12	480	30	2	2.713	2.642	**2.62**
13	720	15	1	2.712	2.681	**1.14**
14	720	15	2	2.713	2.683	**1.11**
15	720	25	1	2.715	2.690	**0.92**
16	720	25	2	2.716	2.692	**0.88**
17	720	30	1	2.714	2.682	**1.18**
18	720	30	2	2.713	2.681	**1.18**

The analysis of the DI values shows an exponential downward trend characteristic of kinetic processes governed by first-order mass transfer, as modeled by the equation of Engh (1992). It is observed that, for the time of 720 s, the variation between replicates is less than 0.05 %, demonstrating excellent repeatability of the RPT test and metrological reliability of the hydrostatic method adopted (D_{RPT}).

The reliability of the DI values calculated is supported by the individual measurement of D_{atm} and D_{RPT} for each replicate of the 18 experimental runs, as shown in Table 4, eliminating the systematic error associated with the use of constant theoretical density. The D_{atm} variability between conditions (2.701–2.716 g/cm³) is consistent with small variations in chemical composition and temperature throughout the tests, and was duly captured by the individualized calculation of the DI.

The results demonstrate a progressive reduction of the Density Index (DI) throughout the degassing process, evidencing the decrease in the potential for gaseous porosity with the increase in the treatment time. As the DI was recalculated using the actual atmospheric density of each experimental condition (D_{atm}), the values

CC BY

REMUNOM
ISSN 2178-6925

Received: 15/10/2026 - **Accepted:** 09/11/2026
Vol: 13.23
DOI: 10.66104/zkvyrq84
Pages: 1-31

presented reflect the effective response of the samples submitted to the RPT test, without dependence on a constant theoretical density of the alloy.

The greatest reduction in DI occurs in the early stages of the process, a behavior compatible with the greater driving force for reduction in RPT-based porosity potential when its concentration in the metal bath is still high. In subsequent cycles, the reduction becomes progressively smaller, characterizing asymptotic behavior typical of diffusive processes of gas removal in liquid metals.

From a practical point of view, the optimal condition should be defined based on the shortest degassing time capable of reaching DI lower than the acceptance criterion established for the process. For HPDC applications, DI values below 2% are generally adopted as a reference for good metallurgical quality, while values close to or below 1% indicate a more stringent condition, suitable for components with high tightness requirements.

4.1.1 Metallographic Analysis of the Samples (Keller Attack)

Four representative conditions of the degassing process were analyzed, corresponding to the times of 0 s, 300 s, 480 s and 720 s, with apparent densities of 1.984 g/cm³, 2.576 g/cm³, 2.676 g/cm³ and 2.713 g/cm³, respectively.

The 0 s specimen was collected before initiation of the DOE campaign and is presented exclusively for qualitative comparison purposes. It was not included in the factorial design, statistical analyses, ANOVA calculations, or response-surface modeling.

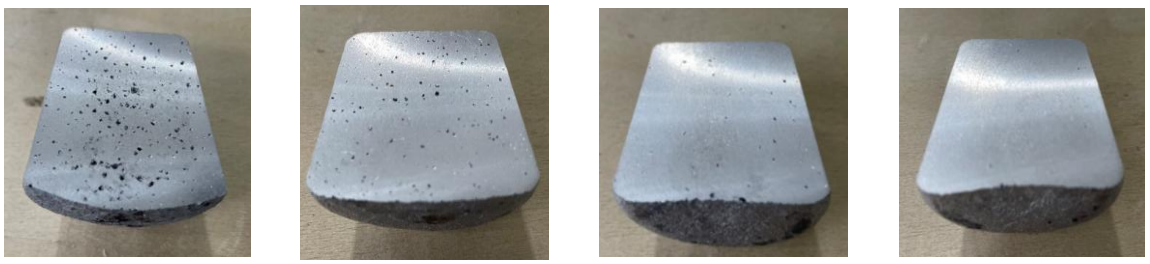
The analysis of the micrographs shows a clear microstructural evolution throughout the process. In the untreated sample (0 s), a high fraction of gaseous porosity was observed, characterized by cavities of varying sizes and heterogeneous distribution, compatible with the high Density Index (DI) previously observed.

Optical microscopy at 100× was used to compare pore morphology among representative conditions. At this magnification and without SEM/EDS confirmation, the images support qualitative description of pores and microstructural contrast but do not permit unequivocal identification of individual intermetallic phases.

CC BY

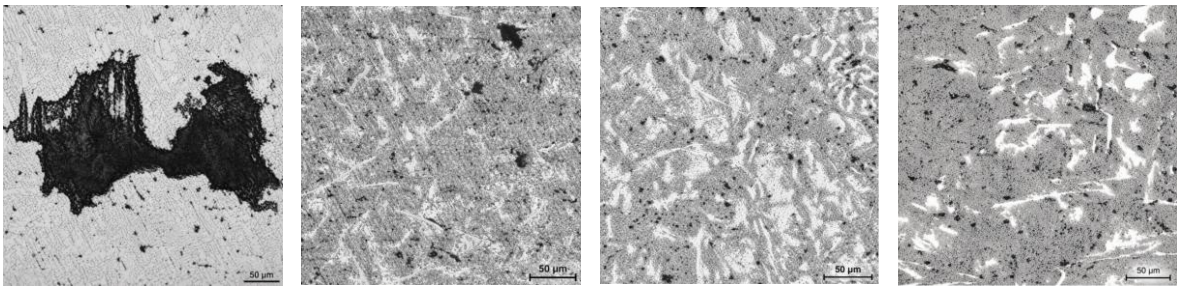
REMUNOM
ISSN 2178-6925

Received: 15/10/2026 - **Accepted:** 09/11/2026
Vol: 13.23
DOI: 10.66104/zkvyrq84
Pages: 1-31



0 s | 1.984 g/cm³ 300 s | 2.576 g/cm³ 480 s | 2.676 g/cm³ 720 s | 2.713 g/cm³

Fig. 2. Side-by-side macroscopic specimen photographs at nominal times; labels give reported specimen density (g/cm³). These ancillary specimens are not traceable to DOE records.



0 s | 1.984 g/cm³ 300 s | 2.576 g/cm³ 480 s | 2.676 g/cm³ 720 s | 2.713 g/cm³

Fig. 3. Side-by-side optical micrographs at nominal times (reported 100×, Keller etch). Original scale bars are retained; no quantitative pore fraction or DOE linkage is asserted.

The metallographic observations are qualitatively consistent with the reduction in DI. Because direct hydrogen measurement and quantitative image analysis were not performed, the images are used as supporting evidence of pore evolution rather than as proof of a unique causal relationship with hydrogen.

4.2 Influence of Bath Temperature on Hydrogen Solubility and treatment response evaluated by DI

The analysis of the experimental data reveals that, in addition to the investigated process parameters (time and flow), the temperature of the metal bath plays a fundamental role in the thermodynamics of degassing.

The solubility of hydrogen in liquid aluminum is governed by Sieverts' Law, according to which the concentration of dissolved hydrogen at equilibrium is proportional to the square root of the partial pressure of hydrogen at the gas-metal interface (ANYALEBECHI, 2022). The dependence of solubility on temperature can be expressed by the Van't Hoff relation, according to Equation (3):

$$\log S = \left(\frac{-2700}{T}\right) + 2.72 \quad (3)$$

CC BY

REMUNOM
ISSN 2178-6925

Received: 15/10/2026 - **Accepted:** 09/11/2026
Vol: 13.23
DOI: 10.66104/zkvyrq84
Pages: 1-31

where S is the equilibrium solubility of hydrogen in pure aluminum at a hydrogen partial pressure of 1 atm and T is absolute temperature (ENGH, 1992). Equation (3) is not a complete equilibrium description of the industrial AA 380.0 bath. Actual hydrogen pickup and equilibrium also depend on alloy composition, hydrogen partial pressure, atmospheric moisture, temperature, and gas–metal interfacial conditions. The calculation is therefore used only to illustrate the temperature trend, not to predict the absolute hydrogen concentration in the experimental alloy.

Applying Equation (3) to the extreme temperatures recorded in this study, the following equilibrium solubility values are obtained for pure aluminum:

- at 787 °C (1060 K): S ≈ 1.49 cm³/100 g;
- at 711 °C (984 K): S ≈ 0.95 cm³/100 g.

This variation represents a reduction of approximately 36% in the equilibrium solubility of hydrogen, due exclusively to the temperature drop of the bath. It is important to note that, for alloys of the Al-Si-Cu system, such as AA 380.0, the presence of silicon and copper reduces the solubility of hydrogen in relation to pure aluminum, with correction factors of the order of 0.6 to 0.8 reported in the literature (ANYALEBECHI, 2022). Nevertheless, the thermodynamic trend remains the same: the reduction in temperature decreases the equilibrium solubility and, consequently, favors the supersaturation of hydrogen in the bath, increasing the driving force for its diffusion towards the inert gas bubbles.

Thus, the reduction in RPT-based porosity potential efficiency observed experimentally is the result of the combined action of two mechanisms:

a) the transfer of convective mass promoted by the injection of inert gas (primary degassing mechanism); and
b) the reduction of the equilibrium solubility of hydrogen with the decrease of the bath temperature (thermodynamic contribution).

This coupling between kinetic and thermodynamic effects explains, in part, the asymptotic behavior observed in the final degassing cycles: as the melt quality response evaluated by the Density Index approaches a plateau (reduced by the lower

CC BY

REMUNOM
ISSN 2178-6925

Received: 15/10/2026 - **Accepted:** 09/11/2026
Vol: 13.23
DOI: 10.66104/zkvyrq84
Pages: 1-31

temperature), the driving force for mass transfer progressively decreases, resulting in marginal efficiency gains.

Bath temperature was recorded as part of routine process monitoring; however, individual temperature values for all experimental runs were not retained in the available dataset. Consequently, temperature could not be incorporated as a statistical covariate in the response surface model and its influence was evaluated qualitatively based on the observed thermal trend.

*4.2.1 Hydrogen Reabsorption Risk (*Regassing*)*

A critical thermodynamic aspect that must be considered in industrial practice is the risk of hydrogen reabsorption (*regassing*) after degassing treatment. At the end of the process, the liquid metal is in a condition of subsaturation in relation to hydrogen, that is, the dissolved gas content is lower than the thermodynamic equilibrium corresponding to the temperature of the bath. This condition creates a driving force favorable to the reabsorption of hydrogen from external sources. The main sources of *regassing* include:

- contact with humid atmosphere during metal transfer to the injection machine;
- tools, shells and gutters with residual moisture or degraded coating;
- metal reheating in the maintenance furnace, which increases the equilibrium solubility of hydrogen, widening the gradient for absorption;
- extended residence time between the end of degassing and the pouring.

According to Sieverts' Law, reheating the metal from 711 °C to 787 °C would raise the equilibrium solubility by approximately 57%, creating thermodynamic conditions highly favorable to hydrogen reabsorption. Therefore, it is recommended that the transfer and pouring of the degassed metal be carried out in the shortest possible time, minimizing exposure to moisture sources and avoiding unnecessary reheating of the bath (GYARMATI et al., 2021; SAMUEL et al., 2023).

This aspect reinforces the importance of considering not only the degassing parameters (time and flow), but also the thermal and logistical management of the treated metal as an integral part of the metallurgical quality control strategy in the HPDC process.

CC BY

REMUNOM
ISSN 2178-6925

Received: 15/10/2026 - **Accepted:** 09/11/2026
Vol: 13.23
DOI: 10.66104/zkvyrq84
Pages: 1-31

4.2.2 Practical interpretation of degassing kinetics

The reduction in RPT-based porosity potential achieved by inert-gas treatment is commonly described using first-order mass-transfer concepts, but quantitative application requires reliable values for bubble diameter, gas hold-up, bath geometry, and mass-transfer coefficients (DISPINAR; CAMPBELL, 2004b; STARCZEWSKI et al., 2025). These variables were not measured in the present industrial campaign. In particular, the previously assumed 5 mm bubble diameter had no experimental basis and has been removed. The kinetic discussion is therefore restricted to qualitative interpretation of the observed diminishing returns with treatment time and flow. The response-surface model remains an empirical model within the investigated factor region and should not be interpreted as a mechanistic bubble-scale model.

The statistical analysis of the results indicated that the degassing time factor presented statistical significance (p-value < 0.05), evidencing its direct influence on the Density Index (DI) of aluminum.

The increase in degassing time promotes greater interaction between the inert gas and the liquid metal, increasing the probability of hydrogen diffusion into the bubbles and their subsequent removal. In terms of DI, the data show that the time of 480 s is sufficient to reach DI values lower than 2.5%, while 720 s allows to achieve DI ≈ 1.0%, meeting the strictest criteria in the international literature for HPDC components with tightness requirements (SAMUEL et al., 2023; VANDER VOORT, 2007).

The statistical analysis confirmed that degassing time was the dominant factor affecting DI, followed by gas flow rate and the time × flow interaction. The high F statistic of the time factor confirms the metallurgical hypothesis that reduction in RPT-based porosity potential is predominantly controlled by the duration of bath exposure to inert gas, in agreement with the first-order kinetic model proposed by Engh (1992). The significance of the interaction reinforces the recommendation of joint optimization of the parameters, avoiding the isolated optimization of a single practical variable frequently reported as generating Regassing or excessive gas consumption in industry (GYARMATI et al., 2021).

CC BY

REMUNOM
ISSN 2178-6925

Received: 15/10/2026 - **Accepted:** 09/11/2026
Vol: 13.23
DOI: 10.66104/zkvyrq84
Pages: 1-31

4.3 Assessment of the suitability of the model – *Lack of Fit Test*

In addition to the analysis of variance of the principal effects, the Lack of Fit test was conducted with the objective of verifying the statistical adequacy of the second-order polynomial model adjusted by the response surface methodology (RSM). This procedure is widely used in publishable experimental planning, as it allows the evaluation of whether the adjusted equation adequately represents the behavior of the experimental data within the investigated region.

The test decomposes the residual error into two parts: pure error, resulting exclusively from the variability observed between replicates, and lack of fit, associated with the inadequacy of the model. As the present study used a 3² factorial design with two replicates per condition, totaling 18 experimental runs, it was possible to perform this statistical decomposition.

The adjusted second-order polynomial model is presented in Equation (4):

$$DI = 12.256 - 0.02305T + 0.01419V \\ +1.007 \times 10^{-5}T^2 - 1.367 \times 10^{-3}V^2 + 3.863 \times 10^{-5}T \cdot V \quad (4)$$

where DI is the Density Index (%), T is the degassing time (s) and V is the inert gas flow rate (L/min).

From the adjusted polynomial model, the stationary point was obtained by the simultaneous resolution of the partial derivatives $\partial DI/\partial T = 0$ and $\partial DI/\partial V = 0$, resulting in $T_{opt} \approx 715$ s and $V_{opt} \approx 24.2$ L/min, with an estimated DI of 0.87 %. This point is in excellent agreement with the experimental values of runs 15 and 16 (DI = 0.88–0.92%), demonstrating the predictive capacity of the model. The Hessian criterion evaluated in the second derivatives ($\partial^2 DI/\partial T^2 > 0$ and $\partial^2 DI/\partial V^2 < 0$) characterizes the point as a smooth saddle point within the factorial region, indicating that the flow has a concave quadratic character (saturation) while the time has a convex quadratic character (asymptotic kinetics), a behavior physically consistent with the kinetic interpretation presented.

CC BY

REMUNOM
ISSN 2178-6925

Received: 15/10/2026 - **Accepted:** 09/11/2026
Vol: 13.23
DOI: 10.66104/zkvyrq84
Pages: 1-31

Table 5. Complete analysis of variance with error decomposition (Lack of Fit)

Source of variation	DF	SQ	MS	F calculated	p-value
Model (RSM)	5	75.1359	15.0272	162.28	< 0.0001
Residual	12	1.1112	0.0926	—	—
Lack of Fit	3	1.0157	0.3386	31.91	< 0.0001
Pure Error	9	0.0955	0.0106	—	—
Total	17	76.2470	—	—	—

Fit quality indicators are presented in Table 6.

Table 6. Indicators of quality of the adjustment

Statistics	Value
R^2	98.54 %
R^2 adjusted	97.94 %
R^2 predicted	96.87 %
PRESS	2.3874

The adjusted polynomial model showed high explanatory power, with R^2 = 98.54%, adjusted R^2 = 97.94% and predicted R^2 = 96.87%, showing excellent ability to describe and predict experimental results. The model showed high global statistical significance ($p < 0.0001$), confirming that at least one of the terms is statistically relevant to describe the variation of the Density Index.

The statistical significance of the lack of fit test must be interpreted in light of the physical nature of the phenomenon itself: the reduction in RPT-based porosity potential in liquid aluminum exhibits first-order kinetics governed by $C_H(t) = C_{H,0} \cdot \exp(-k_L \cdot a \cdot t)$, as described by first-order mass-transfer concepts (ENGH, 1992). Therefore, second-order polynomial models suitable for the study of trends and operational optimization present, by construction, intrinsic limitations in systems governed by exponential equations. Future studies should consider the application of nonlinear models (exponential, logarithmic or hyperbolic), or even the use of transformations in the response variable (e.g., ln(DI)), with a view to suppressing the residual curvature responsible for the Lack of Fit. Despite this limitation, the predicted R^2 of 96.87% demonstrates that the model explains a large proportion of the observed variance. However, the significant lack-of-fit indicates that the polynomial model

CC BY

REMUNOM
ISSN 2178-6925

Received: 15/10/2026 - **Accepted:** 09/11/2026
Vol: 13.23
DOI: 10.66104/zkvyrq84
Pages: 1-31

should be interpreted as an empirical approximation valid only within the investigated experimental region.

4.4 Graphical analysis of the main effects and response surface

In order to complement the statistical analysis of the factors evaluated, graphs of principal effects and a three-dimensional response surface (*Response Surface Methodology* – RSM) were prepared for the Density Index (DI) variable. This approach allows the simultaneous visualization of the effects of degassing time and gas flow on the metallurgical response of the process, enabling the identification of the most favorable operating conditions within the experimental region investigated. The response surface was constructed from a second-order polynomial model adjusted to the experimental results obtained in the 3² factorial design.

4.4.1 Mathematical model of the response surface

The response surface methodology was used to quantitatively describe the influence of the factors degassing time (T) and inert gas flow (V) on the Density Index (DI).

The polynomial model used is represented by the general form in Equation (5):

$$DI = \beta_0 + \beta_1 T + \beta_2 V + \beta_{11} T^2 + \beta_{22} V^2 + \beta_{12} TV \quad (5)$$

where:

- DI = Density Index (%);
- T = degassing time (s);
- V = inert gas flow rate (L/min);
- β_0 = independent term;
- β_1 and β_2 = linear coefficients;
- β_{11} and β_{22} = quadratic coefficients;
- β_{12} = interaction coefficient.

The model coefficients were determined by multiple regression using the least squares method. The statistical significance of the terms included in the model was evaluated by analysis of variance (ANOVA), presented in Table 4, which confirmed

CC BY

REMUNOM
ISSN 2178-6925

Received: 15/10/2026 - **Accepted:** 09/11/2026
Vol: 13.23
DOI: 10.66104/zkvyrq84
Pages: 1-31

the statistically significant influence of the degassing time, gas flow rate, and the interaction between both factors ($p < 0.05$).

The response surface obtained shows that the reduction of the Density Index is strongly associated with the increase in the degassing time, while the effect of the flow rate is less pronounced within the range studied. The observed behavior indicates the existence of an optimal region characterized by high treatment times and intermediate flows, a condition in which the lowest DI values are obtained and, consequently, the highest efficiency of reduction in RPT-based porosity potential from the metal bath.

Figure 4 shows the three-dimensional response surface adjusted by the mathematical model.

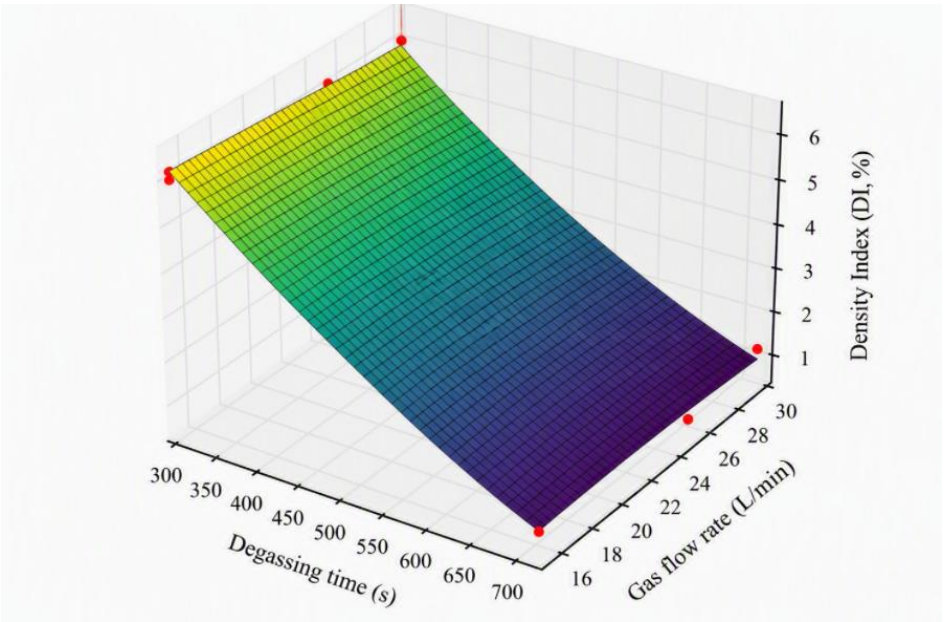


Fig. 4. Response surface (RSM) relating degassing time, gas flow and Density Index (DI).

4.5 Comparison with published degassing and melt-quality studies

Published investigations report DI reductions with increasing degassing duration, but the absolute DI values depend strongly on alloy, initial melt quality, treatment device, filtration, gas dispersion, bath temperature, and sampling practice (DISPINAR; CAMPBELL, 2004a; DISPINAR; CAMPBELL, 2004b; ENGH, 1992; TALBOT; ANYALEBECHI, 1988). The present experiment showed mean DI values of approximately 6.0% at 300 s, 2.8–4.0% at 480 s, and 0.9–1.2% at 720 s across the

CC BY

REMUNOM
ISSN 2178-6925

Received: 15/10/2026 - **Accepted:** 09/11/2026
Vol: 13.23
DOI: 10.66104/zkvyrq84
Pages: 1-31

investigated flow rates. These results follow the general literature trend of rapid initial improvement followed by diminishing returns. Direct numerical ranking against rotary or filtered systems is not appropriate because this study used a RDU and did not measure hydrogen concentration, bubble size, inclusion content, or Bifilm Index. The comparison is therefore limited to trend consistency and process context.

4.5.1 Metallurgical interpretation of results

The relationship between gaseous porosity and mechanical performance in HPDC has been the subject of extensive recent research. Kang et al. (2025) highlight that the control of the hydrogen level and the morphology of porosity is decisive for the structural integrity and tightness of components produced by HPDC. Doty et al. (2025) reinforce that the combination of argon degassing, modification by Sr and grain refining by B represent the current state of the art for improving the mechanical properties of Al-Si alloys.

The results obtained confirm the classic behavior of degassing in aluminum alloys, in which reduction in RPT-based porosity potential occurs more intensely in the initial stages of treatment, followed by a progressive reduction in efficiency in subsequent cycles. This behavior is evidenced by the gradual increase in RPT density and by the reduction of the porosity potential observed in the analyzed samples. The quantitative interpretation of the Density Index (DI), however, should be performed exclusively with the values corrected from the actual atmospheric density (D_{atm}) of each experimental condition.

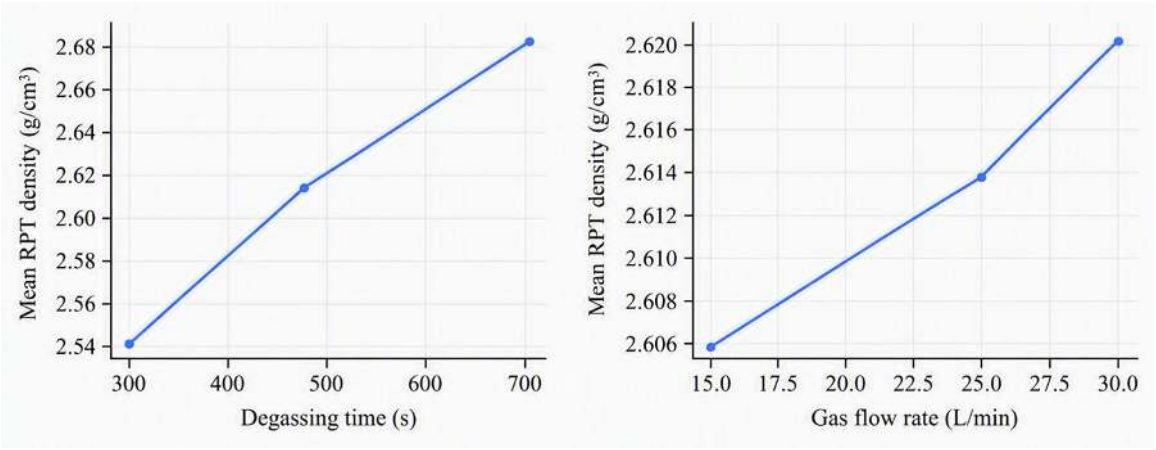


Fig. 5. Density in relation to flow rate and degassing time.

CC BY

REMUNOM
ISSN 2178-6925

Received: 15/10/2026 - **Accepted:** 09/11/2026
Vol: 13.23
DOI: 10.66104/zkvyrq84
Pages: 1-31

The observed DI evolution is directly associated with the decrease of gaseous porosity in the material, which implies improvement of structural integrity and potential increase in the tightness of the components produced by HPDC. The final DI of 1.0% obtained in this work is compatible with the values reported by (DISPINAR; CAMPBELL, 2004a; SAMUEL et al., 2023; VANDER VOORT, 2007) for A356 alloys degassed by rotary degassing, and by Starczewski et al. (2025) for Al-Si eutectic alloys, demonstrating the adequacy of the process to the best practices of the foundry industry.

Additionally, the thermodynamic analysis presented in Section 4.2 demonstrated that the temperature drop of the bath during the process contributes synergistically to the reduction of DI, through the decrease of the equilibrium solubility of hydrogen. This effect, although beneficial during degassing, imposes logistical constraints on the industrial process, since the metal must be transferred and poured in a timely manner to avoid reheating and consequent risk of regassing.

The absence of significant gain in DI with the increase in flow rate above 15 L/min reinforces the importance of optimized control of process parameters, avoiding excessive gas consumption and possible negative impacts on metal quality, including the incorporation of aluminum oxide (Al_2O_3) bifilms, which can act as nucleation sites for internal defects during solidification in the HPDC mold.

4.5.2 Limitations of the Industrial RDU Configuration

Although an industrial Rotary Degassing Unit (RDU) was employed in this study, several limitations must be acknowledged when interpreting the results and comparing them with other published investigations. The present work focused on the evaluation of process performance through the Density Index (DI) and Response Surface Methodology (RSM), whereas important hydrodynamic and metallurgical variables associated with rotary degassing were not directly measured.

In rotary degassing systems, treatment efficiency is strongly influenced by factors such as rotor geometry, rotor wear condition, rotational speed, gas dispersion pattern, bubble size distribution, gas hold-up, and gas-metal interfacial area. These parameters affect mass-transfer rates between the molten metal and the injected inert gas and therefore influence the reduction of porosity potential. In the present study,

CC BY

REMUNOM
ISSN 2178-6925

Received: 15/10/2026 - **Accepted:** 09/11/2026
Vol: 13.23
DOI: 10.66104/zkvyrq84
Pages: 1-31

rotor speed, immersion depth, and gas flow rate were controlled; however, bubble characteristics and interfacial area were not experimentally quantified.

Furthermore, the Density Index (DI) was used as the primary response variable. Although DI is widely accepted as an industrial indicator of melt quality, it represents the porosity potential observed under Reduced Pressure Test (RPT) conditions and should not be interpreted as a direct measurement of dissolved hydrogen concentration. The absence of direct hydrogen measurements, bifilm quantification, K-mold cleanliness evaluation, or inclusion characterization limits the ability to establish the individual contribution of each metallurgical mechanism to the observed improvement in melt quality.

Another limitation is related to bath temperature variation during the experimental campaign. Although temperature was monitored and maintained within the industrial operating range, a progressive temperature reduction occurred throughout the experimental sequence, contributing to the thermodynamic reduction in hydrogen solubility. Because individual temperature measurements for all runs were not retained, temperature could not be incorporated as a covariate in the statistical model. Consequently, the fitted response surface should be interpreted as an empirical representation of the combined effects observed under the experimental conditions investigated.

Therefore, the results presented in this study should be interpreted as evidence of a substantial reduction in RPT-based porosity potential achieved under the tested RDU operating conditions. Direct quantitative comparison with results reported for other rotary degassing systems should be performed with caution, since differences in rotor design, bath geometry, alloy chemistry, treatment practices, filtration conditions, and melt cleanliness can significantly affect the absolute DI values obtained. Future work should incorporate direct hydrogen measurements, quantitative characterization of bubble dispersion, melt-cleanliness assessment techniques, and validation through mechanical or radiographic testing of cast components.

4.6 Industrial Implications

From a practical point of view, the results of this study indicate that:

CC BY

REMUNOM
ISSN 2178-6925

Received: 15/10/2026 - **Accepted:** 09/11/2026
Vol: 13.23
DOI: 10.66104/zkvyrq84
Pages: 1-31

a) the degassing time has a strong influence on the evolution of the RPT density and, consequently, on the improvement of the metallurgical quality of the bath;
b) the gas flow rate should also be considered in the control of the process, especially in conjunction with the degassing time, since the interaction between the factors can alter the experimental response;
c) the definition of the optimal process condition should not be based only on the highest density value, but also on compliance with the criteria of corrected DI, productivity, gas consumption, thermal stability and risk of hydrogen reabsorption;
d) the optimal operating range should be defined based on the combination of metallurgical performance and industrial viability, avoiding both insufficient treatments and excessive process times.

These conclusions allow the optimization of the degassing process, reducing cycle time and resource consumption, without compromising the metallurgical quality of aluminum.

4.7 Originality and contribution of the work

Recent literature emphasizes the influence of gas dispersion, treatment configuration, and combined refining practices on aluminum melt quality (CAMPBELL, 2003; DISPINAR; CAMPBELL, 2004b; GYARMATI et al., 2021; KANG et al., 2025; SAMUEL et al., 2023). The contribution of this work is the replicated statistical evaluation of time and gas flow for an industrial rotary degassing unit (RDU) configuration in AA 380.0, together with explicit definition of the method limitations.

5. Conclusion

The present study evaluated the effect of degassing time and nitrogen flow rate on the RPT-based Density Index of AA 380.0 aluminum alloy processed for HPDC applications. The results showed that increasing degassing time strongly reduced DI, with the lowest experimental values obtained at 720 s and 25 L/min.

The ANOVA analysis with *Lack of Fit* decomposition confirmed that the degassing time is the most statistically relevant factor ($F = 3573.06$; $p < 0.0001$), followed by the gas flow rate ($F = 35.83$) and the time × flow interaction ($F = 26.60$).

CC BY

REMUNOM
ISSN 2178-6925

Received: 15/10/2026 - **Accepted:** 09/11/2026
Vol: 13.23
DOI: 10.66104/zkvyrq84
Pages: 1-31

The Response Surface Methodology model adjusted a second-order polynomial with R^2 = 98.54%, adjusted R^2 = 97.94% and predicted R^2 = 96.87%. The fitted polynomial provides a useful empirical representation of the experimental trends; however, the significant lack-of-fit indicates that nonlinear models may provide a more adequate description of the process.

The density results indicated a progressive increase in the RPT density with the increase in the degassing time, evidencing a reduction in the potential for gaseous porosity and an improvement in the metallurgical quality of the bath. The statistical interpretation of the factors degassing time, gas flow and time × flow interaction should be supported by the ANOVA presented in the body of the article, using the response variable effectively analyzed.

Gas flow rate was statistically significant within the studied design, and its effect depended on treatment time, as indicated by the significant time × flow interaction. The lowest observed DI occurred at 720 s and 25 L/min; increasing flow to 30 L/min did not improve DI at 720 s, indicating diminishing returns within the tested range.

Within the studied factor region, 720 s and approximately 25 L/min produced the lowest DI values. The 480 s conditions did not meet DI < 1%, so they should not be grouped with the 720 s condition as equivalent. The RSM stationary point is an empirical estimate inside the experimental region and should be validated independently before use as an industrial standard operating condition.

As original scientific contributions, this work presents:

(i) the quantification of the treatment response evaluated by DI by nitrogen in AA 380.0 under strict statistical criteria (ANOVA + RSM + *Lack of Fit*);

(ii) the integration between first-order kinetics (ENGH, 1992) and Sieverts thermodynamics for coupled interpretation of the process;

(iii) the critical discussion of the limitations of the system in the face of contemporary RDU technologies.

Limitations of the present work include the absence of direct hydrogen measurement, the absence of K-mold inclusion cleanliness testing, the lack of direct radiographic validation of finished HPDC parts, and the lack of mechanical testing.

CC BY

REMUNOM
ISSN 2178-6925

Received: 15/10/2026 - **Accepted:** 09/11/2026
Vol: 13.23
DOI: 10.66104/zkvyrq84
Pages: 1-31

Although an industrial RDU was employed, bubble characteristics and gas-metal interfacial area were not experimentally quantified. Consequently, the results should be interpreted as RPT/DI-based evidence of reduced porosity potential within the process window studied, rather than as a complete qualification of structural performance. As a recommendation for future studies, the following are indicated: (a) the application of the same DOE in an RDU system for direct comparison between technologies; (b) the use of nonlinear kinetic models for a more accurate representation of the observed asymptotic behavior; (c) the inclusion of SEM/EDS chemical microanalysis to confirm intermetallic phases; (d) direct correlation between DI and mechanical properties in HPDC components produced under the optimized conditions; and (e) K-mold or equivalent melt-cleanliness assessment.

A limitation of the present work is that bath temperature was not incorporated as an experimental factor in the DOE or as a statistical covariate during model fitting.

Funding Declaration

This research received no specific grant from any funding agency in the public, commercial, or not-for-profit sectors.

Ethics approval

Not applicable.

References

Anyalebechi, P. N. “Hydrogen Solubility in Liquid and Solid Pure Aluminum – Critical Review of Measurement Methodologies and Reported Values.” *Materials Sciences and Applications*, vol. 13, 2022, pp. 158–212, https://doi.org/10.4236/msa.2022.134011.

ASTM International. *ASTM B85/B85M-18: Standard Specification for Aluminum-Alloy Die Castings*. ASTM International, 2018, https://doi.org/10.1520/B0085_B0085M-18E01.

CC BY

REMUNOM
ISSN 2178-6925

Received: 15/10/2026 - **Accepted:** 09/11/2026
Vol: 13.23
DOI: 10.66104/zkvyrq84
Pages: 1-31

ASTM International. *ASTM B962-23: Standard Test Methods for Density of Compacted or Sintered Powder Metallurgy Products Using Archimedes' Principle*. ASTM International, 2023, https://doi.org/10.1520/B0962-23.

ASTM International. *ASTM E155-20: Standard Reference Radiographs for Inspection of Aluminum and Magnesium Castings*. ASTM International, 2020, https://doi.org/10.1520/E0155-20.

Campbell, J. *Castings*. 2nd ed., Butterworth-Heinemann, 2003.

Dispinar, D., and J. Campbell. "Critical Assessment of Reduced Pressure Test. Part 1: Porosity Phenomena." *International Journal of Cast Metals Research*, vol. 17, 2004, pp. 280–286, https://doi.org/10.1179/136404604225020696.

Dispinar, D., and J. Campbell. "Critical Assessment of Reduced Pressure Test. Part 2: Quantification." *International Journal of Cast Metals Research*, vol. 17, 2004, pp. 287–294, https://doi.org/10.1179/136404604225020704.

Doty, H. W., et al. "Effect of Melt Treatment and Heat Treatment on the Performance of Aluminum Cylinder Heads." *Materials*, vol. 18, 2025, article 1024, https://doi.org/10.3390/ma18051024.

Engh, T. A. *Principles of Metal Refining*. Oxford UP, 1992.

Gyarmati, G., et al. "The Effects of Rotary Degassing Treatments on the Melt Quality of an Al-Si Casting Alloy." *International Journal of Metalcasting*, vol. 15, 2021, pp. 141–151, https://doi.org/10.1007/s40962-020-00428-z.

ISO. *ISO/IEC 17025:2017: General Requirements for the Competence of Testing and Calibration Laboratories*. International Organization for Standardization, 2017.

Kang, Hj., et al. "Effects of Porosity on Mechanical Properties of Castings in High-Pressure Die-Casting Process." *International Journal of Metalcasting*, vol. 19, 2025, pp. 2918–2927, https://doi.org/10.1007/s40962-024-01520-4.

CC BY

REMUNOM
ISSN 2178-6925

Received: 15/10/2026 - **Accepted:** 09/11/2026
Vol: 13.23
DOI: 10.66104/zkvyrq84
Pages: 1-31

Lazaro-Nebreda, J., et al. “Degassing of Aluminum Alloy Melts by High Shear Melt Conditioning Technology: An Overview.” *Metals*, vol. 12, 2022, article 1772, https://doi.org/10.3390/met12101772.

Merchan, M., et al. “High-Pressure Die Casting Process Parameters Optimization for Al-Mg-Fe Aluminum Alloy Structural Parts Manufacturing.” *Metals*, vol. 15, 2025, article 1071, https://doi.org/10.3390/met15101071.

Piekos, M., and Z. Smorawinski. “Introduction of Powder Fluxes in Rotary Degassing System towards Intensifying Refining Process of Aluminium Alloys.” *Archives of Foundry Engineering*, vol. 24, 2024, pp. 89–94, https://doi.org/10.24425/afe.2024.151315.

Samuel, A. M., et al. “A Review on Porosity Formation in Aluminum-Based Alloys.” *Materials*, vol. 16, 2023, article 2047, https://doi.org/10.3390/ma16052047.

Starczewski, J., et al. “Evaluation of the Technological Properties of the Al-Si Eutectic Alloy Based on Density Index Test.” *Archives of Foundry Engineering*, vol. 25, 2025, https://doi.org/10.24425/afe.2025.155349.

Szymczak, T., et al. “The Effect of Changes in Degassing Parameters on Gasification and Crystallization of EN AC-46000 Alloy.” *Archives of Foundry Engineering*, vol. 25, 2025, pp. 124–132, https://doi.org/10.24425/afe.2025.155389.

Talbot, D. E. J., and P. N. Anyalebechi. “Solubility of Hydrogen in Liquid Aluminium.” *Materials Science and Technology*, vol. 4, 1988, pp. 1–4, https://doi.org/10.1179/mst.1988.4.1.1.

Vander Voort, G. F. *Metallography: Principles and Practice*. ASM International, 2007.

Wang, Y., et al. “Investigating Synergistic Mechanisms of Porous Injection-Flux for Aluminum Melt Purification.” *Metallurgical and Materials Transactions B*, 2026, https://doi.org/10.1007/s11661-026-08229-5.

CC BY